AGU PUBLICATIONS

Water Resources Research

RESEARCH ARTICLE

10.1002/2017WR020442

Key Points:

- Model input data reduction using the Discrete Wavelet Transform
- Rainfall is estimated using model inversion techniques
- Simultaneous estimation of rainfall and model parameters improves model performance

Correspondence to:
A. J. Wright,
ashley.wright@monash.edu

Citation:
Wright, A. J., J. P. Walker, and V. R. N. Pauwels (2017), Estimating rainfall time series and model parameter distributions using model data reduction and inversion techniques, *Water Resour. Res.*, *53*, 6407–6424, doi:10.1002/2017WR020442.

Received 23 JAN 2017
Accepted 7 JUL 2017
Accepted article online 13 JUL 2017
Published online 1 AUG 2017

Estimating rainfall time series and model parameter distributions using model data reduction and inversion techniques

Ashley J. Wright[1], **Jeffrey P. Walker**[1], **and Valentijn R. N. Pauwels**[1]

[1]Department of Civil Engineering, Monash University, Clayton, Victoria, Australia

Abstract Floods are devastating natural hazards. To provide accurate, precise, and timely flood forecasts, there is a need to understand the uncertainties associated within an entire rainfall time series, even when rainfall was not observed. The estimation of an entire rainfall time series and model parameter distributions from streamflow observations in complex dynamic catchments adds skill to current areal rainfall estimation methods, allows for the uncertainty of entire rainfall input time series to be considered when estimating model parameters, and provides the ability to improve rainfall estimates from poorly gauged catchments. Current methods to estimate entire rainfall time series from streamflow records are unable to adequately invert complex nonlinear hydrologic systems. This study aims to explore the use of wavelets in the estimation of rainfall time series from streamflow records. Using the Discrete Wavelet Transform (DWT) to reduce rainfall dimensionality for the catchment of Warwick, Queensland, Australia, it is shown that model parameter distributions and an entire rainfall time series can be estimated. Including rainfall in the estimation process improves streamflow simulations by a factor of up to 1.78. This is achieved while estimating an entire rainfall time series, inclusive of days when none was observed. It is shown that the choice of wavelet can have a considerable impact on the robustness of the inversion. Combining the use of a likelihood function that considers rainfall and streamflow errors with the use of the DWT as a model data reduction technique allows the joint inference of hydrologic model parameters along with rainfall.

1. Introduction

Floods can have significant economic, social, and environmental impacts [*Brouwer and Van Ek*, 2004]. Cost benefit analyses and environmental and social impact assessments are common evaluation methods available to water policy decision makers [*Hajkowicz and Collins*, 2007]. Flood forecast skill greatly influences societal resilience to floods. However, without accurate, precise, and timely rainfall information, the value of such analytical tools is rendered subjective.

Currently, rainfall uncertainty is the biggest obstacle hydrologists face in their pursuit toward obtaining accurate, precise, and timely flood forecasts [*McMillan et al.*, 2011]. Operational flood forecasters tend to adhere to familiar flood forecasting procedures, including semidistributed event-based hydrological models [*Pagano et al.*, 2009]. Consequently, it is often not possible for reliable flood forecasts to be issued until the catchment's response to rainfall has been observed [*Elliott*, 1997]. Hydrologists look to overcome this by using continuous hydrological models, but the lack of reliable rainfall inputs from quantitative precipitation forecasts (QPFs) impedes the development of robust flood forecasts [*Hapuarachchi et al.*, 2011]. *Robertson et al.* [2013] and *Shrestha et al.* [2015] have demonstrated that skill can be added to raw QPFs by postprocessing the raw QPFs using past observations as input into a methodology that combines a simplified version of the Bayesian joint probability with the Schaake Shuffle [*Clark et al.*, 2004]. The Schaake Shuffle is a methodology to reconstruct space-time variability in forecasted precipitation and temperature fields. The combination of the use of model input data reduction techniques with parameter estimation algorithms allows links to be explored between rainfall input error, QPF postprocessing algorithms, and errors associated with model structure, parameter estimation, and systematic and random errors associated with observations.

Due to complex interactions between Hortonian overland flow, saturation excess overland flow, interflow, and groundwater flow, discrepancies are quite often noticed between similar rainfall events and the corresponding runoff, and vice versa. Hence, the process of estimating rainfall from streamflow observations is an ill-posed problem. As a large proportion of hydrologists favor deterministic models [*Pappenberger and Beven*, 2006], it is not surprising that some attempts to estimate rainfall from runoff have taken a deterministic rather than probabilistic approach [*Hino*, 1986; *Kirchner*, 2009]. While using analytical inversion to estimate rainfall from streamflow, *Kirchner* [2009] draws attention to the fact that, of the components of the water balance, only streamflow can be considered a catchment-scale observation. Hence, the authors ask, can streamflow and/or soil moisture be used to estimate catchment-scale rainfall time series?

The root zone soil moisture state can have a large impact on a catchment's rainfall-runoff characteristics [*Grayson et al*., 2006]. Recent studies [e.g., *Crow*, 2007; *Pellarin et al*., 2008; *Crow et al*., 2009, 2011; *Kucera et al*., 2013; *Pellarin et al*., 2013; *Brocca et al*., 2014] focus on using soil moisture to correct and estimate rainfall accumulations. *Brocca et al*. [2014] coined the phrase "*Soil as a Natural Rain Gauge*." In the Soil Moisture to Rain (SM2RAIN) algorithm [*Brocca et al*., 2014], rainfall estimates are retrieved from the inversion of the soil water balance equation, assuming that all rainfall infiltrates. *Ciabatta et al*. [2015] uses the SM2RAIN algorithm to nudge satellite precipitation estimates in order to estimate daily rainfall; *Abera et al*. [2016] validates this product in a comparative study. If rainfall estimates that are based on a satellite soil moisture product are to be used in a flood forecasting situation, it is imperative that the rainfall estimate is up to date and that the satellite soil moisture images are obtained immediately prior to the flood. With the continued improvement of satellite rainfall and soil moisture measurement missions, such as the Global Precipitation Measurement (GPM) mission [*Hou et al*., 2014] and the Soil Moisture Active Passive (SMAP) [*Entekhabi et al*., 2010] mission, it is expected that the methods outlined by *Crow et al*. [2011], *Brocca et al*. [2014], and *Ciabatta et al*. [2015] will become more valuable for estimating rainfall time series in the future. Yet there are currently no methods that use both streamflow and soil moisture to estimate rainfall [*Kavetski et al*., 2006a, 2006b; *Vrugt et al*., 2008; *Renard et al*., 2010, 2011]. Rainfall estimation methods that solely rely on streamflow measurements maintain good temporal resolution, yet have been subject to poor performance in catchments that have complex rainfall-runoff characteristics and exhibit highly nonlinear rainfall-runoff behavior. In an early attempt to estimate rainfall from streamflow, *Hino* [1986] separated time series of daily discharge into their respective runoff components using coefficients obtained from fitting an Auto-Regressive Moving Average (ARMA) model. Using the law of parsimony, otherwise known as Occam's razor—"*Entities should not be multiplied unnecessarily*"—*Kirchner* [2009], *Teuling et al*. [2010], *Adamovic et al*. [2015], and *Rusjan and Mikoš* [2015] used first-order approximations to analytically invert the water balance equation. These approximations also assume that all rainfall infiltrates and are not able to estimate rainfall when streamflow is generated by other mechanisms. Using the Bayesian Total Error Analysis (BATEA) framework [*Kavetski et al*., 2006a], *Kavetski et al*. [2006b] are able to estimate rainfall time series by identifying storms within a rainfall time series and estimating a storm multiplier that acts to modify each of the observations within that storm. Using a Markov Chain Monte Carlo (MCMC) sampler known as the Differential Evolution Adaptive Metropolis (DREAM) [*Vrugt et al*., 2009b], *Vrugt et al*. [2008] also estimated rainfall time series using storm multipliers. This methodology results in prediction uncertainty bounds for storm events as well as significantly altering the posterior parameter distributions for the hydrological model parameters. Work by *Renard et al*. [2010, 2011] have built on the idea of using storm multipliers by using rainfall multipliers characterized by a hyperdistribution. The importance of specifying informative prior distributions on rainfall errors was demonstrated. Additionally, conditional simulation was proposed as an effective method to build such priors for daily rainfall estimation. Using multiplicative error structures for rainfall has shown promise, yet is unable to ascertain uncertainty when no rainfall is recorded. This is a critical gap that has not been addressed in literature, particularly for poorly gauged catchments. Depending on the location of a rainfall gauge, poorly gauged catchments are particularly prone to overestimate, underestimate, or completely miss localized rainfall. Thus, it is imperative that a characterization of rainfall error allows for uncertainty that is independent of the observed rainfall magnitude to be developed. Further, rainfall observations of the same magnitude may have different uncertainty. The use of transfer functions to reduce input model data into parameters allows for a window of input data to be adjusted for each parameter. In contrast to the use of storm multipliers, the use of transfer functions allows for uncertainty in rainfall events to be accounted for when no rainfall is recorded at the gauge.

This paper explores the use of wavelets to estimate rainfall time series in the context of a lumped catchment-scale rainfall-runoff model. To address the need for estimating rainfall time series, this paper will address (i) the use of the DWT to reduce model input data to parameters for estimation of input uncertainty,

(ii) possible methodologies to estimate input uncertainty using DWTs and DREAM$_{(ZS)}$, and (iii) estimation of rainfall input series and the validation of results against rainfall and streamflow observations.

2. Hydrologic Model Description

For this study, the Sacramento Soil Moisture Accounting (SAC-SMA) model was used with a fixed integration time step of 1 day. This lumped conceptual watershed model is used by the National Weather Service River Forecast System (NWSRFS) for flood forecasting throughout the United States. This model has been used as well to model the rainfall-runoff transformation throughout Australia [*Herron et al*., 2002] and has shown promising results for soil moisture data assimilation [*Crow and Ryu*, 2009].

The SAC-SMA model can be described as a nonlinear regression model, $\mathcal{F}(\cdot)$, which simulates a n-record of discharge values, $\mathbf{Y}=\{y_1,\ldots,y_n\}$ in mm/d:

$$\mathbf{Y}=\mathcal{F}(\boldsymbol{\theta},\tilde{\mathbf{x}}_0,\hat{\mathbf{E}},\hat{\mathbf{R}}). \tag{1}$$

The model input arguments are the $1\times d$ vector, $\boldsymbol{\theta}$ with SAC-SMA parameter values, the $1\times m$ vector $\tilde{\mathbf{x}}_0$ with values of the initial states (at $t=0$) in mm, and $1\times n$ vectors $\hat{\mathbf{E}}=\{\hat{e}_1,\ldots,\hat{e}_n\}$ and $\hat{\mathbf{R}}=\{\hat{r}_1,\ldots,\hat{r}_n\}$ that store the observed values of the potential evapotranspiration (PET) and rainfall in mm/d, respectively. Note, the $\hat{}$ (hat) symbol is used to denote measured quantities, and a $\tilde{}$ (tilde) symbol reflects variables that could, in theory, be observed in the field but due to their conceptual nature are difficult to determine accurately.

The SAC-SMA model is comprised of three layers: surface, upper, and lower soil moisture layers. A variable impervious area alters the percentage of precipitation that contributes to direct runoff and infiltration into the upper soil layer. Evapotranspiration is able to occur from surface water as well as the lower and upper zone tension water stores. The upper soil layer is comprised of tension and free water. For free water to be able to contribute to the lower zone via percolation, total channel flow via interflow or surface runoff, the tension water store must first be full. Losses in tension water through evapotranspiration can be replenished by free water in both the lower and upper soil layers. The lower soil layer is comprised of tension water as well as primary and supplementary free water stores. Unlike the upper layer, the lower layer has a reserve on the percentage of free water that can supplement tension water losses due to evapotranspiration. Both the primary and supplementary free water stores contribute to a primary and supplementary base flow. A portion of base flow contributes to the total channel flow, whilst another portion contributes to subsurface discharge. For a more detailed description of the SAC-SMA model, the reader is referred to *NWS* [2002].

Based on the recommendations of *Peck* [1976], the 16 parameter SAC-SMA model has been reduced to 13 parameters by fixing SIDE, RIVA, and RSERV, the parameters that control the ratio of deep recharge to channel base flow, Riparian vegetation area, and fraction of lower zone free water not transferable to lower zone tension water, respectively. Consequently, the SAC-SMA model used has 13 parameters and 6 state variables, hence, $d=13$ and $m=6$. The parameter distribution for the remaining 13 parameters is obtained using the DREAM$_{(ZS)}$ algorithm [*Laloy and Vrugt*, 2012; *Vrugt*, 2016]. The initial parameter space was selected based on recommendations by *Boyle et al*. [2000]. Since the Maximum A Posteriori Probability (MAP) solution involved a large number of parameters that were hitting their respective upper or lower bound, adjustments of the parameter space were made based on recommendations of *Anderson et al*. [2006]. Even with these more relaxed ranges, some parameters continued to find their MAP value at the edge of their respective search domains. For those parameters, the search ranges were further increased—making sure that values remain physically plausible. Table 1 summarizes the parameters of the SAC-SMA model including their prior uncertainty ranges. Note, these enlarged ranges of the parameters are justified given the rather contrasting characteristics of the Warwick catchment as compared to the watersheds studied by *Boyle et al*. [2000] and *Anderson et al*. [2006].

3. Bayesian Inference of SAC-SMA Model Parameters and Rainfall Time Series

The rainfall-runoff parameter estimation problem has been studied extensively in the literature. Many different approaches have been developed to find the optimal parameter estimates. These approaches initially focused on finding only the global optimal values of the parameters for some given objective function [*Duan et al*., 1994; *Gan and Biftu*, 1996; *Thyer et al*., 1999]. In the past two decades, the interest has switched

Table 1. Parameters of the SAC-SMA Model and the Range Used for the Estimation Process

Parameter	Description	Units	Initial Range
Capacity Thresholds			
UZTWM	Upper zone tension water capacity	mm	1.00–150.00
UZFWM	Upper zone free water capacity	mm	1.00–150.00
LZTWM	Lower zone tension water capacity	mm	10.00–500.00
LZFPM	Lower zone free water primary capacity	mm	$10.00-1.00\times10^{4}$
LZFSM	Lower zone free water supplemental capacity	mm	5.00–400.00
Recession Parameters			
UZK	Upper zone free water withdrawal rate	day^{-1}	$1.00\times10^{-1}-7.50\times10^{-1}$
LZPK	Lower zone primary free water withdrawal rate	day^{-1}	$1.00\times10^{-4}-2.50\times10^{-2}$
LZSK	Lower zone supplemental free water withdrawal	day^{-1}	$1.00\times10^{-2}-8.00\times10^{-1}$
Percolation			
ZPERC	Maximum percolation rate		1.00–500.00
REXP	Exponent of the percolation equation		1.00–5.00
PFREE	Fraction percolation from upper to lower zone free water storage		$0.00-8.00\times10^{-2}$
Impervious Area			
PCTIM	Minimum impervious fraction of the watershed area		$0.00-1.00\times10^{-1}$
ADIMP	Additional impervious area		$0.00-4.00\times10^{-1}$
Fixed Parameters			
RIVA	Riparian vegetation area		0.00
SIDE	Ratio of deep recharge to channel base flow		0.00
RSERV	Fraction of lower zone free water not transferable to tension water		3.00×10^{-1}

to assessment of parameter and prediction uncertainty. Examples of such methods include Bayesian recursive parameter estimation [*Thiemann et al.*, 2001], the limits of acceptability approach [*Beven*, 2006; *Blazkova and Beven*, 2009], the Bayesian Total Error Analysis (BATEA) framework [*Kavetski et al.*, 2006a, 2006b; *Kuczera et al.*, 2006; *Thyer et al.*, 2009; *Renard et al.*, 2011], the Simultaneous Optimization and Data Assimilation (SODA) [*Vrugt et al.*, 2005], the DREAM algorithm and its variations [*Vrugt et al.*, 2005, 2008, 2009a, 2009b; *Vrugt and Ter Braak*, 2011; *Laloy and Vrugt*, 2012; *Sadegh and Vrugt*, 2014], Bayesian model averaging [*Butts et al.*, 2004; *Ajami et al.*, 2007; *Vrugt and Robinson*, 2007], the hypothetico-inductive data-based mechanistic modeling framework of *Young* [2013], and Bayesian data assimilation [*Bulygina and Gupta*, 2011]. This paper adopts a Bayesian viewpoint to quantify model parameter and predictive uncertainty. If the SAC-SMA parameters, initial states, PET, and rainfall are considered to be unknown, then their posterior probability distribution, $p(\boldsymbol{\theta},\tilde{\mathbf{x}}_0,\tilde{\mathbf{E}},\tilde{\mathbf{R}}|\hat{\mathbf{Y}},\hat{\mathbf{E}},\hat{\mathbf{R}})$ can be estimated from the observed discharge, PET, and rainfall time series using Bayes Law

$$p(\boldsymbol{\theta},\tilde{\mathbf{x}}_0,\tilde{\mathbf{E}},\tilde{\mathbf{R}}|\hat{\mathbf{Y}},\hat{\mathbf{E}},\hat{\mathbf{R}})=\frac{p(\boldsymbol{\theta},\tilde{\mathbf{x}}_0,\tilde{\mathbf{E}},\tilde{\mathbf{R}})L(\boldsymbol{\theta},\tilde{\mathbf{x}}_0,\tilde{\mathbf{E}},\tilde{\mathbf{R}}|\hat{\mathbf{Y}},\hat{\mathbf{E}},\hat{\mathbf{R}})}{p(\hat{\mathbf{Y}},\hat{\mathbf{E}},\hat{\mathbf{R}})}, \tag{2}$$

where the $p(\boldsymbol{\theta},\tilde{\mathbf{x}}_0,\tilde{\mathbf{E}},\tilde{\mathbf{R}})$ signifies the joint prior distribution of the parameters, initial states, potential evapotranspiration, and rainfall, respectively, $L(\boldsymbol{\theta},\tilde{\mathbf{x}}_0,\tilde{\mathbf{E}},\tilde{\mathbf{R}}|\hat{\mathbf{Y}},\hat{\mathbf{E}},\hat{\mathbf{R}})$ denotes the likelihood function, and the denominator $p(\hat{\mathbf{Y}},\hat{\mathbf{E}},\hat{\mathbf{R}})$ represents the evidence or the marginal likelihood. This formulation of Bayes law takes into consideration explicitly the major sources of uncertainty involved in the modeling of the rainfall-runoff transformation. Indeed, rainfall and PET observations are subject to considerable uncertainty, and if their errors are not properly treated then the SAC-SMA parameters will compensate, in part, for their misspecification.

The prior distribution, $p(\boldsymbol{\theta},\tilde{\mathbf{x}}_0,\tilde{\mathbf{E}},\tilde{\mathbf{R}})$ summarizes all the information about the SAC-SMA parameters, initial states, potential evapotranspiration, and rainfall data records and their multivariate dependencies before the primary data (hydrologic measurements) and/or secondary data (watershed characteristics) are collected. The likelihood function quantifies in probabilistic terms the distance between the observed and simulated data. Finally, the evidence, $p(\hat{\mathbf{Y}},\hat{\mathbf{E}},\hat{\mathbf{R}})$ normalizes the posterior distribution so that it integrates to unity, and represents a proper statistical distribution. This constant is independent of the parameter values; hence, the marginal likelihood can be removed from equation (2) and a proportionality sign used instead

$$p(\boldsymbol{\theta},\tilde{\mathbf{x}}_0,\tilde{\mathbf{E}},\tilde{\mathbf{R}}|\hat{\mathbf{Y}},\hat{\mathbf{E}},\hat{\mathbf{R}})\propto p(\boldsymbol{\theta},\tilde{\mathbf{x}}_0,\tilde{\mathbf{E}},\tilde{\mathbf{R}})L(\boldsymbol{\theta},\tilde{\mathbf{x}}_0,\tilde{\mathbf{E}},\tilde{\mathbf{R}}|\hat{\mathbf{Y}},\hat{\mathbf{E}},\hat{\mathbf{R}}) \tag{3}$$

Equation (3) considers joint inference of the parameters of the SAC-SMA model, its initial states, and rainfall and potential evapotranspiration data records. This would involve the estimation of a very large number of unknowns, and result in issues such as overfitting.

To proceed, the following is taken advantage of

1. Watershed-scale hydrologic processes exhibit generative, negative feedbacks that gravitate the moisture status to a stable state, also called attractor. Numerical results of watershed models indeed demonstrate that the effect of the initial states on the model results rapidly diminishes with increasing "distance" from the start of simulation. Therefore, advantage can be taken of a spin-up period of Q days to remove sensitivity of the modeling results and error residuals to state value initialization.
2. The inherent low-pass filter properties of watershed models and buffer capacity of soil moisture stores cause the governing state dynamics and output fluxes to be relatively insensitive to random and systematic errors in the PET data [*Oudin et al.*, 2006; *Samain and Pauwels*, 2013], and it can be conveniently assumed that $\delta_t(\tilde{\mathbf{E}}_{(t-\Delta t:t)}, \mathbf{E}_{(t-\Delta t:t)}) \approx 0$. Yet the framework presented herein can be easily extended to explicitly treat errors in PET observations as well.

If these two assumptions are adopted, then equation (3) simplifies to

$$p(\boldsymbol{\theta}, \tilde{\mathbf{R}}|\hat{\mathbf{Y}}, \hat{\mathbf{R}}) \propto p(\boldsymbol{\theta}, \tilde{\mathbf{R}}) L(\boldsymbol{\theta}, \tilde{\mathbf{R}}|\hat{\mathbf{Y}}, \hat{\mathbf{R}}). \tag{4}$$

It can further safely be assumed that the prior information of the parameters and rainfall record are independent. Thus, the multivariate joint prior distribution, $p(\boldsymbol{\theta}, \hat{\mathbf{R}})$, can be replaced with two individual prior distributions for the parameters and the hyetograph. If it is further assumed that the prior parameter distribution, $p(\boldsymbol{\theta})$ is uniform, flat, and noninformative, then this leaves the following definition of the posterior distribution, $p(\boldsymbol{\theta}, \tilde{\mathbf{R}}|\hat{\mathbf{Y}}, \hat{\mathbf{R}})$, of the parameters and rainfall record given the observed discharge and rainfall record. Equation (4) can be further simplified by decomposing the likelihood function into two separate likelihood functions for the discharge data and rainfall record as follows: $L(\boldsymbol{\theta}, \tilde{\mathbf{R}}|\hat{\mathbf{Y}}, \hat{\mathbf{R}}) = L(\boldsymbol{\theta}|\hat{\mathbf{Y}}) L(\boldsymbol{\theta}|\hat{\mathbf{R}})$. This decomposition is appropriate as it is highly plausible that the rainfall and discharge measurement data errors are independent. Thus, the following equation remains

$$p(\boldsymbol{\theta}, \tilde{\mathbf{R}}|\hat{\mathbf{Y}}, \hat{\mathbf{R}}) \propto p(\tilde{\mathbf{R}}) L(\boldsymbol{\theta}|\hat{\mathbf{Y}}) L(\boldsymbol{\theta}|\hat{\mathbf{R}}), \tag{5}$$

and requires the user to define the rainfall data prior, $p(\tilde{\mathbf{R}})$, and the pair of likelihood functions, $L(\boldsymbol{\theta}|\hat{\mathbf{Y}})$, and $L(\boldsymbol{\theta}|\hat{\mathbf{R}})$, respectively. Before the mathematical definition of these three distributions is further discussed, the parameterization of the rainfall record is presented. This is of crucial importance and prerequisite to the numerical implementation of equation (5).

4. Model Input Data Reduction Using the DWT

Wright et al. [2017] provided a comparison of the discrete wavelet and discrete cosine transforms for hydrologic model input data reduction and recommended that the Discrete Wavelet Transform be used for hydrologic studies that have both short and long temporal durations that also involve rainfall as an input. Using the pyramid algorithm developed by *Mallat* [1989] along with the Daubechies wavelets [*Daubechies*, 1990] an input rainfall signal can be transformed into a set of rainfall parameters. This algorithm can be summarized as follows. The input rainfall $\tilde{\mathbf{R}}$ is passed through high- and low-pass filters where

$$\mathbf{p}_j^{\mathrm{L}}(i) = \begin{cases} \sum_{m=1}^{\mathrm{L}} \tilde{\mathbf{R}}(2i-m-1)\mathrm{w}(m), & j=1 \\ \sum_{m=1}^{\mathrm{L}} \mathbf{p}_{j-1}^{L}(2i-m-1)\mathbf{w}(m), & j>1. \end{cases} \tag{6}$$

is the low pass and

$$\mathbf{p}_j^{\mathrm{H}}(i) = \begin{cases} \sum_{m=1}^{\mathrm{L}} \tilde{\mathbf{R}}(2i-m-1)\mathrm{h}(m), & j=1 \\ \sum_{m=1}^{\mathrm{L}} \mathbf{p}_{j-1}^{L}(2i-m-1)\mathrm{h}(m), & j>1. \end{cases} \tag{7}$$

is the high pass, where $\mathrm{h}(m)$ and $\mathrm{w}(m)$ are the scaling and wavelet functions used in the high- and low-pass filters, respectively. $\mathbf{p}_j^{\mathrm{L}}(i)$ and $\mathbf{p}_j^{\mathrm{H}}(i)$ refer to the low- and high-pass parameters at the jth level, respectively.

This process decomposes the original signal into levels of parameters that preserve resolution in both the temporal and frequency domains. Due to the length of each resultant parameter series being equivalent to the length of the input series, every other parameter is removed to avoid redundancy. This process is referred to as down sampling. At this stage, further decomposition can be achieved by iteratively passing the low-pass parameters through the filtering equations. At each level, the low- and high-pass parameters can be referred to as approximation or detail parameters. A number of different combinations of these DWT approximation and detail parameters can be sampled to alter different components of the rainfall time series. After the parameters are sampled, the DWT decomposition process is reversed by iterating through

$$\mathbf{p}_{j-1}(i)=\sum_{m=\lceil i/2\rceil}^{\lfloor (\mathrm{L}-1+i)/2\rfloor}(\mathbf{p}_j^{\mathrm{H}}(i)\mathrm{h}(2m-i))(\mathbf{p}_j^{\mathrm{L}}(i)\mathrm{w}(2m-i)),\quad j>1, \tag{8}$$

where $\lceil . \rceil$ is the ceiling operator. Finally, the input signal is reconstructed using

$$\tilde{\mathbf{R}}(i)=\sum_{m=\lceil i/2\rceil}^{\lfloor (\mathrm{L}-1+i)/2\rfloor}(\mathbf{p}_j^{\mathrm{H}}(i)\mathbf{h}(2m-i))(\mathbf{p}_j^{\mathrm{L}}(i)w(2m-i)),\quad j=1, \tag{9}$$

before the resulting rainfall time series is able to passed into equation (5) for evaluation. A major advantage of using discrete wavelet decomposition is that the user is able to alter the number of parameters used to sample the posterior rainfall time series. As more levels of decomposition are used, a lower number of approximation parameters describe the low-pass component of the rainfall time series. One drawback of estimating the approximation parameters with more levels of decomposition is that lower resolution can be achieved. For a more detailed discussion on the DWT, the reader is referred to *Mallat* [2009].

5. Formulation of Posterior Distribution

Now that a sparse parameterization for the rainfall record has been defined, there remains the definition for the prior distribution, $p(\tilde{\boldsymbol{R}})$ and two likelihood functions, $L(\boldsymbol{\theta}|\hat{\mathbf{Y}})$ and $L(\boldsymbol{\theta}|\hat{\mathbf{R}})$, in equation (5), respectively. In this paper, the inference results for a formulation of the posterior distribution of equation (5) is presented to evaluate the sensitivity of the posterior distribution to the underlying assumptions regarding the information content of the discharge and rainfall data.

The formulation of $p(\boldsymbol{\theta},\tilde{\mathbf{R}}|\hat{\mathbf{Y}},\hat{\mathbf{R}})$ in equation (5) is derived from *Kavetski et al.* [2006a] and assumes a Gaussian likelihood for $L(\boldsymbol{\theta}|\hat{\mathbf{Y}})$ and $L(\boldsymbol{\theta}|\hat{\mathbf{R}})$, respectively,

$$L(a|b)=-\frac{1}{2}n\log\left(\sum_{t=1}^{n}(a_t-b_t)^2\right), \tag{10}$$

with n-input vectors, a and b. Using $\boldsymbol{\beta}$ to describe the ratio of the n rainfall depths (in mm/day) predicted by the k wavelet parameters and their corresponding measured values where,

$$\boldsymbol{\beta}=\left\{\frac{\tilde{r}_1}{\hat{r}_1},\ldots,\frac{\tilde{r}_n}{\hat{r}_n}\right\}, \tag{11}$$

a vague inverse gamma prior for $p(\tilde{\boldsymbol{R}})$ is used

$$p(\sigma_{\boldsymbol{\beta}}^2|v_0,s_0)\propto\frac{1}{\sigma_{\boldsymbol{\beta}}^{v_0+1}}\exp\left(-\frac{v_0s_0^2}{2\sigma_{\boldsymbol{\beta}}^2}\right), \tag{12}$$

where $\sigma_{\boldsymbol{\beta}}$ (mm/d) signifies the rainfall measurement data error, and $v_0>0$ $s_0>0$ (mm/d) are the scale and shape parameter of the inverse gamma prior, respectively.

If the prior of equation (12) is combined with the Gaussian likelihoods of the rainfall and discharge data record then the following formulation of the posterior distribution in equation (5) is derived:

$$p(\boldsymbol{\theta},\tilde{\mathbf{R}}|\hat{\mathbf{Y}},\hat{\mathbf{R}})\propto\left[\mathrm{SSE}(\boldsymbol{\beta},1)+v_0s_0^2\right]^{-\frac{k+v_0-1}{2}}\mathrm{SSE}(\mathbf{Y}(\boldsymbol{\theta}),\hat{\mathbf{Y}})^{-\frac{n}{2}}, \tag{13}$$

where $\mathrm{SSE}(a,b)=\sum_{t=1}^{n}(a-b)^2$ and $\mathbf{Y}(\boldsymbol{\theta})=\mathcal{F}(\boldsymbol{\theta},\tilde{\mathbf{x}}_0,\tilde{\mathbf{E}},\tilde{\mathbf{R}})$.

If any of the n rainfall multipliers deviate from unity then the first term on the right-hand side (likelihood of rainfall data) decreases. This is only acceptable if the value of the discharge likelihood (second term, right-hand side) increases sufficiently such that posterior density increases as a whole. Thus, the formulation of equation (13) constrains the rainfall adjustments as large changes to the measured rainfall record are discouraged, unless the fit to the discharge data increases so much so that the product of the two likelihoods increases.

In practice, it is much more convenient to work with the log-formulation of equation (13) as this avoids numerical problems with a zero density if n becomes large. *Kavetski et al*. [2006b] is followed and it is assumed that $v_0=5$ and that the value of s_0 is estimated along with the d model parameters and k wavelet parameters. This thus involves the inference of $k+d+1$ unknowns.

6. Posterior Sampling

A key task in Bayesian inference is now to summarize the posterior distribution of the individual SAC-SMA parameters, and rainfall estimates at times $t=\{1,\ldots,n\}$. Unfortunately, for equation (13), this task cannot be carried out analytically, and thus Markov Chain Monte Carlo (MCMC) simulation with the DREAM$_{(ZS)}$ algorithm to generate samples of the posterior distribution [*Vrugt et al*., 2008, 2009b; *Vrugt*, 2016] is used. This method runs $N \geq 3$ different Markov chains in parallel and proposals in each chain are created using parallel direction and snooker updates from an archive of past states of the chains. Snooker updates involve sampling along an axis that is developed from past states in preference to sampling along the coordinate axis. This approach solves a practical problem in Monte Carlo Markov chain (MCMC) simulation, that is choosing a correct orientation and scale of the proposal distribution. To maximize speed up convergence to the target distribution, the DREAM$_{(ZS)}$ algorithm uses adaptive randomized subspace sampling to only update a random selection of parameters. A detailed description of the DREAM$_{(ZS)}$ algorithm appears in *Laloy and Vrugt* [2012], *Vrugt* [2016], and related cited publications.

For all numerical studies presented herein, default values for the algorithmic parameters [*Vrugt*, 2016] and $N=3$ Markov chains are used. Convergence of the sampled chain trajectories using the $\hat{R}$ convergence diagnostic [*Gelman and Rubin*, 1992] is used. This statistic compares, for each dimension of the target distribution, the variance of each parameter within each chain to the variance of that same parameter between the N different chains. All trials were executed until the $\hat{R}$-diagnostic convergence criterion was smaller than the stipulated threshold of 1.2, $\hat{R}_j \leq 1.2 \;\; \forall \;\; j=\{1,\ldots,k+d+1\}$.

7. Site and Data Description

The data set used for the experiment comprises daily rainfall from 14 operational real-time rain gauges, Potential Evapotranspiration (PET), and observed streamflow data for the Warwick catchment. Warwick is a small subcatchment of the Condamine-Culgoa catchment, Figure 1. Located in South-East Queensland, Australia, the total drainage area for the Warwick catchment is 1360 km^2. The Warwick basin has been subjected to multiple flood events of significant magnitude in the past decade. The total length of the perennial channels is 78 km. Cease to flow conditions have been observed during times of extended drought. The maximum elevation difference along the channel is 308 m. The highest, lowest and mean elevations in the catchment are 1361, 446, and 650 m Above Mean Sea Level (AMSL), respectively. In the period beginning at the start of November 2000 and finishing at the end of June 2015, the mean, median, 10th percentile, and 90th percentile annual rainfall amounts for the Warwick Alert rainfall gauge are 564, 513, 408, and 748 mm/yr, respectively. Due to the severe droughts that affected Australia for most of the first decade of the millennium, it is likely that these rainfall statistics are negatively biased and that, over a longer time period the average rainfall at these gauges would be larger than those observed. The analysis period used the data with highest quality and begins 1 January 2007 and ends 31 March 2013. Areal rainfall is constructed using the Inverse Distance Weighting (IDW) method, which is current operational practice at the Australian Bureau of Meteorology (BoM). Distance is calculated from the catchment centroid to the rain gauge. Monthly PET data from the Australian Water Availability Project (AWAP) were used. A crump weir was used to record continuous height measurements. These height measurements have been converted to streamflow using periodically updated rating curves.

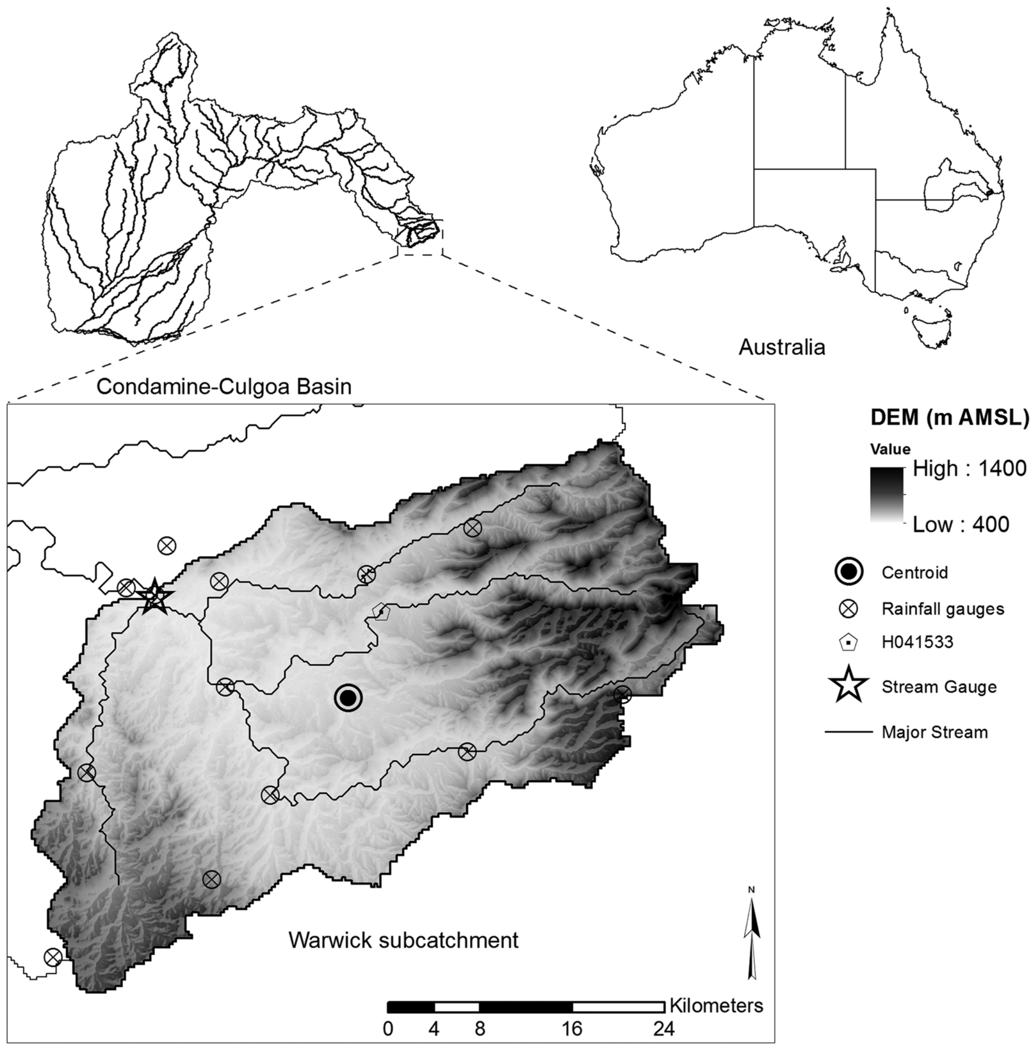

Figure 1. The location of the Condamine-Culgoa basin in Australia and digital elevation map of the Warwick subcatchment within this region. The notation "m AMSL" in the legend denotes "meters above mean sea level."

8. Synthetic Case Study

8.1. Aims

The synthetic case study was designed as a preliminary study to explore some of the different model input data reduction techniques that wavelets make available. A major aim of the synthetic case study was to assess the suitability of the db1 and db2 wavelets to account for a known random multiplicative heteroscedastic Gaussian error. Another aim was to assess the value of rainfall, model parameter, and streamflow estimates using a model parameter estimation approach, a segmented rainfall and model parameter estimation approach, and via the simultaneous estimation of rainfall and model parameters.

8.2. Description of Experiments

As there is no definite true rainfall time series and model parameter set for the Warwick catchment, a synthetic case study was conducted. The DWT was used to reduce model input data, to estimate rainfall time series that are representative of the "synthetic true" rainfall from an imperfect rainfall product. Synthetic streamflow data and model parameters were created by estimating the SAC-SMA model parameters using areal rainfall and observed streamflow. The simulated streamflow, estimated parameters, and areal rainfall are considered to be the synthetic truth. A random multiplicative heteroscedastic Gaussian error with standard deviation equivalent to 10% of the observation was added to the synthetic rainfall truth in order to simulate the errors that can be expected in an areal rainfall product. Evaluating different assumptions of error types and distributions is outside the scope of this study and is a possible direction for future studies. The choice of error does not detract from the ability of the synthetic case study to demonstrate that the DWT is a powerful transform that can be used to estimate rainfall time series. Throughout the synthetic case study, the perturbed rainfall and PET are used as the a priori input data, the synthetic streamflow truth and perturbed rainfall truth are used as the evidence for the posterior estimation of model parameters, rainfall, and streamflow.

Throughout the synthetic case study, rainfall time series were estimated by inverting the estimated level 4 wavelet approximation parameters. The selection of the parameter level to be estimated and analysis wavelet to be used determines the number of rainfall observations that each parameter will impact. The level 4 approximation parameters were chosen to maximize the trade-off between the benefit gained by representing the rainfall data set using DWT parameters and creating a highly dimensionalized problem that cannot feasibly be solved. The DWT transform is used with the Daubechies db1 and db2 wavelets. It is necessary to test different wavelets to assess the impact they have on the assumed error structure. The model was allowed a spin-up period of 100 days. Five years data were used in the calibration period and 357 days of data were used for the validation period. DWT parameters are only estimated in the calibration period, consequently rainfall is only estimated in the calibration period.

The synthetic case study was comprised of four tests and a benchmark. The benchmark synthetic test E simulated streamflow using the perturbed rainfall input and the synthetic truth parameters. Synth 1 used the synthetic true model parameters, and the DWT parameters were then constructed and estimated based on the perturbed input rainfall. The second test, Synth 2, estimated only the SAC-SMA parameters using the perturbed rainfall data. The third and last tests, Synth 3 and Synth 4, simultaneously estimated both the SAC-SMA parameters and the DWT parameters for the perturbed input rainfall using the db1 and db2 wavelets, respectively. During the synthetic case study, only the level 4 approximation parameters were modified. Of which there were 115 and 116 for the db1 and db2 wavelets, respectively.

8.3. Results and Discussion

The performance of each synthetic test in the calibration and validation period as well as the rainfall and streamflow volume for the calibration and validation periods are shown in Table 2. All synthetic experiments apart from Synth 3 were able to simulate streamflow at least as well as the benchmark synthetic test E. The implications of this result will be elaborated on. As there is no observation error in the synthetic truth streamflow and the synthetic true model parameters are known in Synth 1, Synth 1 therefore tests the ability of the proposed methodology to deal with a random heteroscedastic multiplicative Gaussian error in isolation. If subsequent tests are not susceptible to overfitting then, for the given DWT setup, Synth 1 should place a lower bound on the streamflow RMSE able to be achieved in the calibration period. However, as the calculated RMSE in the calibration period for Synth 2 is much lower than the calculated RMSE for Synth 1 and the benchmark test E, it is clear that the model parameters are being modified in order to satisfy the likelihood function.

Surprisingly Synth 3 both simulates streamflow and estimates rainfall the poorest. As the RMSE of streamflow in the calibration period is closely related to the second term of equation (13), the only way that this

Table 2. Description of the Experimental Setup of the Synthetic Case Study Used Herein Along With the Results for the Calibration (Cal) and Evaluation (Val) Periods[a]

Experimental Setup					RMSE Streamflow ($m^3\ s^{-1}$)		Streamflow		Rainfall	
Experiment	Rainfall	Model	Wavelet	Coef	Cal (101:1925)	Val (1926:22,82)	Cal (GL)	Val (GL)	Cal (mm)	Val (mm)
Truth							688.26	75.82	3205.12	544.48
E		N			3.54	1.18	699.73	74.05	3208.07	545.18
S1	Y	N	db1	Appx 4 (115)	3.12	1.20	657.52	72.35	2688.52	545.18
S2	N	Y			2.54	1.09	624.63	68.92	3208.07	545.18
S3	Y	Y	db1	Appx 4 (115)	4.67	11.06	639.00	115.66	1941.30	545.18
S4	Y	Y	db2	Appx 4 (116)	2.39	2.83	644.47	59.07	2902.05	545.18

[a]The rainfall, model, wavelet, and coef columns indicate which parameters are being estimated, the analysis wavelet being used, and which, if any, any wavelet parameters are being estimated. The number of wavelet parameters estimated are shown in brackets. E indicates the simulation in which the perturbed rainfall is used with the synthetic true model parameters; S1, S2, etc. are used to label the synth studies 1, 2, etc. The results in the streamflow and rainfall columns are estimated volumes of that designated period. Rainfall is not modified in the validation period.

Table 3. Comparison of the Synthetic True Parameters to the MAP Solution Alongside the Minimum and Maximum Limits for the Marginal Density for Each Parameter for Two Synthetic Studies

Parameter	Synthetic Truth	Synth 2	Min	Max	Synth 4	Min	Max
Capacity Thresholds							
UZTWM	24.82	30.06	25.75	31.85	79.35	74.19	82.16
UZFWM	11.87	8.67	8.29	9.30	10.18	10.17	10.50
LZTWM	55.63	84.31	79.46	91.30	10.47	10.00	11.34
LZFPM	42.84	23.81	19.86	27.84	139.20	110.66	139.20
LZFSM	8.01	10.94	9.54	12.35	18.57	15.32	20.93
Recession Parameters							
UZK	6.26×10^{-1}	7.50×10^{-1}	7.15×10^{-1}	7.50×10^{-1}	5.32×10^{-1}	5.01×10^{-1}	5.89×10^{-1}
LZPK	6.22×10^{-3}	1.53×10^{-2}	1.17×10^{-2}	1.79×10^{-2}	1.37×10^{-3}	1.01×10^{-3}	1.72×10^{-3}
LZSK	5.26×10^{-1}	5.79×10^{-1}	5.30×10^{-1}	6.24×10^{-1}	5.01×10^{-1}	4.51×10^{-1}	5.66×10^{-1}
Percolation							
ZPERC	497.23	93.12	82.02	127.92	2.07	1.35	4.15
REXP	4.37	5.00	4.95	5.00	4.99	4.98	5.00
PFREE	4.29×10^{-1}	3.86×10^{-1}	3.44×10^{-1}	4.12×10^{-1}	7.74×10^{-1}	7.27×10^{-1}	5.80×10^{-1}
Impervious Area							
PCTIM	1.35×10^{-2}	1.56×10^{-2}	1.11×10^{-2}	1.79×10^{-2}	1.91×10^{-2}	1.67×10^{-2}	2.35×10^{-2}
ADIMP	1.85×10^{-2}	3.40×10^{-5}	2.81×10^{-9}	1.04×10^{-3}	8.29×10^{-4}	6.55×10^{-8}	7.30×10^{-3}

solution can be returned as the MAP solution is that the first term of equation (13) was increased sufficiently so that the resulting posterior density increased. The reason for this is the inability of the db1 wavelet to account for random multiplicative heteroscedastic Gaussian errors. Modification of the DWT level 4 approximation parameters in Synth 3 results in a homogeneous adjustment in rainfall for the window in which the DWT parameter adjusts. Consequently, it is postulated that the db1 wavelet is more suited to correct homoscedastic errors. The validity of this postulation may vary with model structure and distribution of parameters. The good simulation of streamflow and estimation of a realistic rainfall time series in Synth 4, in which the level 4 wavelet parameters for the db2 wavelet are estimated, further validates this observation. The nonlinear nature of the db2 wavelet allows the estimation of wavelet parameters to account for random multiplicative heteroscedastic Gaussian errors.

The 13 SAC-SMA synthetic truth model parameters are compared to the MAP solutions obtained using the perturbed rainfall product and the simultaneous estimation of model parameters as well as rainfall in Table 3. The parameter distributions obtained in Synth 2 and Synth 4 are rarely able to estimate parameter distributions that describe the synthetic truth model parameters. Given the prevalent nature of equifinality in hydrological systems, this result is not all together unexpected. The only difference between the generation of the synthetic truth model parameters and the estimation of model parameters in Synth 2 is that the input rainfall is perturbed with a random heteroscedastic multiplicative Gaussian error. Since the synthetic truth parameters are not able to be estimated, it is expected that the model parameters were erroneously modified in order to account for input error and consequently produce superior streamflow. Consequently, unless either the input error is removed before simulation or additional constraints, such as using informative priors in a similar fashion to *Renard et al*. [2010], are placed on the system, it is likely that estimations of both rainfall and model parameters will include some erroneous modifications in order to satisfy the likelihood function. It is also seen in Synth 4 that even small modifications to input rainfall are able to vastly change the model parameters estimated. This result does not mean that realistic rainfall time series cannot be estimated, but rather that the rainfall time series estimated may include some errors.

Comparisons of the perturbed rainfall, the MAP rainfall estimations using the synthetic true model parameters, and the simultaneous estimation of DWT rainfall parameters and model parameters using the db1 and db2 analysis wavelets are made against the synthetic true rainfall in Figure 2. While the perturbed rainfall was best able to represent the synthetic true rainfall, the rainfall estimations from Synth 1, Synth 3, and Synth 4 were still quite reasonable. Due to the slope of the estimations made by the db2 wavelet being closer to unity than those obtained using the db1 wavelet, the larger coefficient of determination and the lower RMSE, it is evident that the db2 wavelet is more suited to representing the random multiplicative heteroscedastic Gaussian errors than the db1 wavelet. Neither Synth 3 or Synth 4 are able to represent rainfall as well as Synth 1 in which the true model parameters are assumed known. This is further proof that the

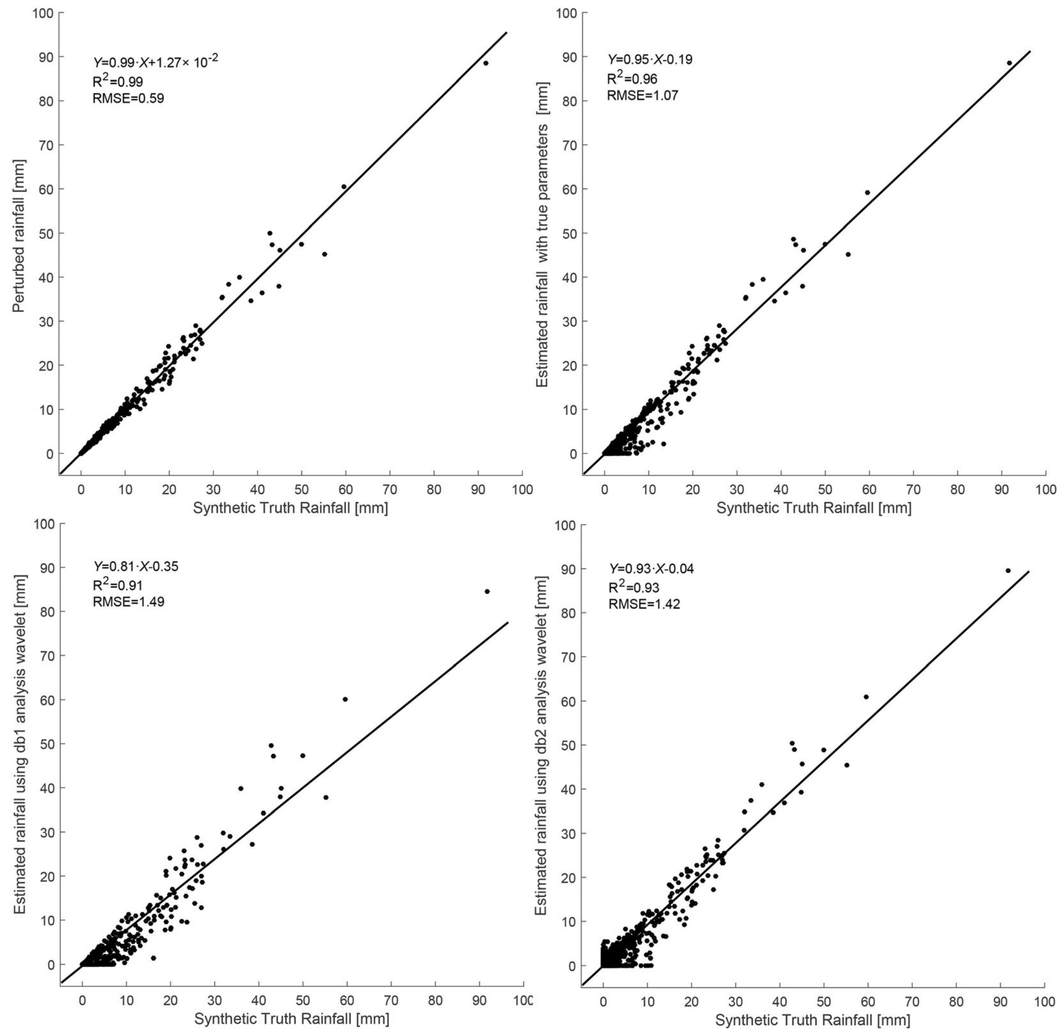

Figure 2. Comparison of the (top left) perturbed synthetic truth rainfall and (top right) synthetic and estimated rainfall using inference of only the wavelet parameters, joint inference of the SAC-SMA model parameters and wavelet parameters using the (bottom left) db1 wavelet and (bottom right) db2 wavelet. The linear least squares fit and corresponding quality of fit metrics are separately indicated in each plot.

rainfall and model parameter estimations can be erroneously modified in order to produce superior streamflow.

Figure 4 supports the hypothesis that rainfall time series can be estimated through the simultaneous modification of DWT rainfall parameters and model parameters. Figure 4 (top) shows the total volume of rainfall estimations over the calibration period for the synthetic experiments 2 and 4 next to benchmark test E. Also shown are the maximum (3945 mm) and minimum (2660 mm) rainfall volumes observed throughout the catchment. Using the true synthetic parameters, S2 is able to estimate a rainfall time series that simulates streamflow better than the benchmark simulation and is in partial agreement with the volumes observed at the rainfall gauges. The rainfall time series estimated in S4 is able to estimate rainfall that has a total volumetric range that is generally in agreement with observations while simulating streamflow with a lower RMSE than the perturbed input product.

The synthetic case study has shown that the db1 wavelet does not adequately account for random multiplicative heteroscedastic Gaussian errors for the described model data reduction and model inversion methodology to estimate rainfall time series. The db2 is a more suitable wavelet choice. A model parameter distribution that describes the synthetic true model parameters could not be retrieved. However, this was not entirely unexpected. A rainfall time series that is generally in agreement with observations could be estimated via the simultaneous estimation of rainfall and model parameters. All rainfall time series estimated using the db2 wavelet led to better simulations than the benchmark test experiment, a traditional calibration approach in which only model parameters are estimated, and the estimation of rainfall time series using the synthetic truth model parameters.

Since the synthetic experiments were applied at a relatively coarse temporal resolution, it is expected that using a finer resolution would enable rainfall estimations to meet or exceed the ability of the perturbed rainfall input to model the synthetic true rainfall. Even if the rainfall estimations are not able to reproduce the synthetic true rainfall, the methodology still has a few advantages in that rainfall time series that are similar, yet in this instance have a drier tendency, to those observed at the gauges are produced. These series are able to simulate streamflow which is closer to the synthetic streamflow than that produced by the synthetic rainfall. Thus, it is likely that streamflow forecasts would benefit from rainfall forecasts that are conditioned on rainfall time series that are known to give good results.

9. Observation Case Study

9.1. Aims

The observation case study was designed to further explore some of the different model input data reduction techniques that wavelets make available. A major aim of the study was to assess the suitability of the db1 and db2 wavelets to account for unknown errors in input data. Other aims were to determine the impacts of estimating approximation and detail parameters at different levels as well as assessing the value of rainfall and streamflow estimates using a traditional calibration approach, a segmented rainfall and model parameter estimation approach and via the simultaneous estimation of rainfall and model parameters. This study does not aim to nor is able to improve streamflow simulations in the validation period but rather aims to gain understanding of realistic representations of rainfall that can lead to superior streamflow simulations.

9.2. Description of Experiments

The observation case study begins by estimating an initial parameter distribution set for the 13 SAC-SMA parameters in experiment 1. Experiment 2 then used the estimated MAP parameter set to estimate a rainfall time series. The main difference between experiments for experiments 2 to 8 is that the DWT is either constructed differently or different parameters of the DWT are being estimated. In experiment 3, simultaneous estimation of model parameter distributions and rainfall time series was then performed by estimating the wavelet approximation parameters, experiments 4 and 5 involved estimating the detail parameters of different levels. To this point, the level of decomposition was held constant throughout. Next, in experiments 6 and 7, the simultaneous estimation of model parameter distributions and rainfall time series was performed by estimating the wavelet approximation parameters under different levels of wavelet decomposition. The number of DWT parameters estimated for each experiment are given in Table 4. After this the simultaneous estimation of model parameter distributions and rainfall time series was conducted in experiment 8 using the "db2" wavelet. This was done to assess the ability of the db1 and db2 wavelet to model the errors for the experiments.

Similar to the synthetic case study, the model was allowed a spin-up period of 100 days, 5 years data were used in the calibration period and 357 days of data were used for the validation period. Throughout the observation case study, observed rainfall and PET are used as the a priori input data, the observed streamflow and rainfall are used as the evidence for the posterior estimation of model parameters, rainfall and streamflow.

9.3. Results and Discussion

The performance of the inference approaches in the observation case study for the calibration and validation period (where applicable) as well as the rainfall and streamflow volume for the calibration and validation periods are shown in Table 4. All of the experiments were able to estimate model parameter and temporal rainfall distributions or combinations thereof that yield superior streamflow simulations in the calibration period. As expected, there was no discernible difference in the validation period. This is because rainfall was not able to be modified in this period.

Table 4. Description of the Experimental Setup of the Observation Case Study Used Herein Along With the Results for the Calibration (Cal) and Evaluation (Val) Periods[a]

Experimental Setup					RMSE Streamflow ($m^3 s^{-1}$)		Streamflow		Rainfall	
Experiment	Rainfall	Model	Wavelet	Coef	Cal (101:1925)	Val (1926:22,82)	Cal (GL)	Val (GL)	Cal (mm)	Val (mm)
T							685.17	195.29	3205.12	544.48
1	N	Y			5.74	37.40	688.26	75.82	3205.12	544.48
2	Y	N	db1	Appx 4 (115)	3.99	37.29	730.27	92.20	2994.80	544.48
3	Y	Y	db1	Appx 4 (115)	3.43	37.39	697.51	77.32	2957.16	544.48
4	Y	Y	db1	Lev 4 (115)	4.23	40.28	704.58	54.84	4470.98	544.48
5	Y	Y	db1	Lev 3 (115)	3.33	41.86	689.15	19.38	4743.98	544.48
6	Y	Y	db1	Appx 5 (229)	3.91	41.69	658.22	16.56	4523.15	544.48
7	Y	Y	db1	Appx 3 (58)	3.21	39.79	721.51	56.60	3149.52	544.48
8	Y	Y	db2	Lev 4 (116)	3.62	37.60	702.91	75.81	3113.49	544.48

[a]The rainfall, model, wavelet, and coef columns indicate which parameters are being estimated, the analysis wavelet being used, and which, if any, wavelet parameters are being estimated. The number of wavelet parameters estimated is shown in brackets. The results in the streamflow and rainfall columns are estimated volumes of that designated period. Rainfall is not modified in the validation period.

While the streamflow simulations are consistently improved, the resulting estimated model parameter distributions and rainfall time series or combinations thereof are not all desirable. In experiment 2, a rainfall time series was estimated using the MAP model parameter set found in experiment 1. Thus, a set of rainfall time series that agrees with the observed gauged rainfall was estimated. In contrast to the synthetic case study (Synth 3 and Synth 2), the simultaneous estimation of both rainfall time series and model parameter distributions in experiment 3 is able to both simulate streamflow better than experiment 2 and produce rainfall time series that are closer to the rainfall observations at the gauges. While the estimated rainfall series from experiments 4, 5, and 6 are able to simulate superior streamflow, the resultant estimated rainfall time series appears to be unrealistic when compared to the volumes at the rainfall gauges.

In general, the results from experiments 3–6 suggest that the use of the wavelet approximation parameters yield superior results when compared to use of the wavelet detail parameters. When compared to solely estimating model parameters, the streamflow simulated in experiments 3 and 7 showed that RMSE improved by a factor of 1.67 and 1.78, respectively. As expected, using a higher level of decomposition and consequently less parameters in the rainfall reduction in experiment 3 did not produce superior streamflow simulations, or rainfall time series when compared to the use of a lower level of decomposition and estimation of more wavelet parameters in experiment 7. The use of the "db2" wavelet in experiment 8 produced similar streamflow simulations and rainfall time series as was found in experiment 3. This finding suggests that, unlike the introduced error in the synthetic case study, errors in rainfall observations may not be of a random heteroscedastic multiplicative Gaussian nature. Studies conducted by *Renard et al*. [2010] and *McMillan et al*. [2011] have attempted to evaluate multiplicative error models and account for input and structural errors in hydrological modeling, respectively. Their findings indicate that rainfall errors, especially in larger storms, appear to be heteroscedastic. A shortcoming of the studies was that errors in rainfall when no rainfall was observed were not taken into account. Consequently, more work is required to determine error models that account for errors when no rainfall is observed. The results of this study indicate that the DWT transform is a tool that can be utilized to further understand rainfall errors. Further work would look at identifying a superior analysis wavelet for the categorization of rainfall errors and rainfall reduction. The unrealistic estimation of rainfall time series in experiments 4–6 further suggests that using informative priors for rainfall measurement error [*Renard et al*., 2010] may produce fruitful results.

A depiction of the estimated rainfall for a 120 day duration is provided in Figure 3 for comparison to other rainfall estimation methods. Unlike the methodology proposed by *Hino* [1986], this method does not attempt to separate streamflow into respective runoff components. Further, as was the case in work conducted by *Kirchner* [2009], *Teuling et al*. [2010], *Adamovic et al*. [2015], and *Rusjan and Mikoš* [2015], no first-order approximations, to ensure the water balance can be analytically inverted, are made. Figure 3 shows that this methodology allows for uncertainty in rainfall to be estimated when no rainfall was observed at the gauges. This is a shortcoming of studies that use the rainfall multiplier method [*Kavetski et al*., 2006a, 2006b; *Vrugt et al*., 2008; *Renard et al*., 2010, 2011]. By using the DWT to describe rainfall, this study attempts to move away from the rainfall multiplier methods. The effectiveness of the study is somewhat limited by

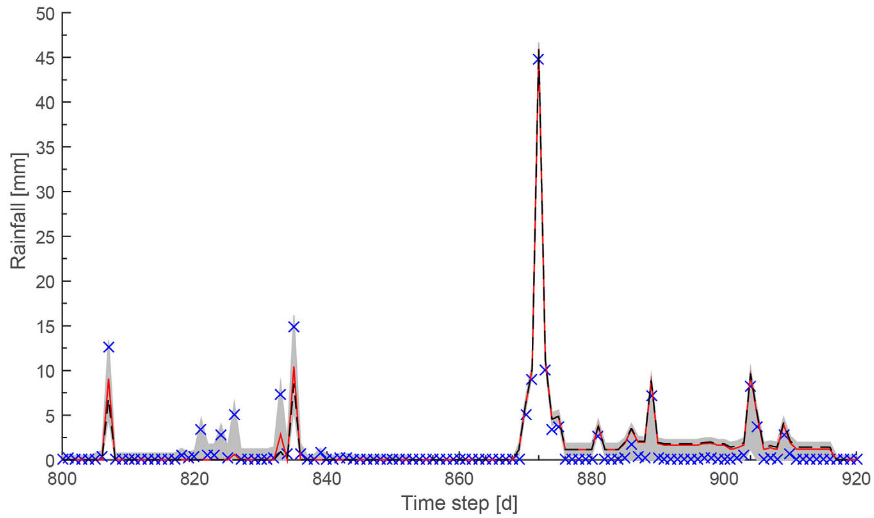

Figure 3. Rainfall estimates for experiment 3 over a 120 day period. The blue crosses and red line represent the observed rainfall and mean rainfall estimates, respectively. The dashed red line is the MAP rainfall estimate while the grey shading indicates the 5th and 95th percentile rainfall estimates.

the use of multipliers in formulation of the likelihood function. Developing a new likelihood function was outside the scope of the paper. Doing so in future studies could enhance the value of the techniques described within this study. Since the resultant streamflow from experiment 3 is superior to that obtained from a traditional calibration approach, the median, MAP 5th and 95th percent rainfall estimates indicate times when streamflow is improved by providing increased or decreased estimates of rainfall as well as the degree of uncertainty associated with the rainfall estimates. It is observed that both the median and MAP rainfall estimates are close to zero when rainfall was observed at the gauge for the time period spanning the 820th to the 830th days. Conversely, rainfall estimates are higher than that observed at the gauge for the time period spanning the 875th to the 885th day. Further, during the time period spanning the 855th to the 865th day, the rainfall estimates completely agree with the observations of zero rainfall. This finding indicates that the rainfall estimation methodology, when applied to the SAC-SMA model, is able to account for rainfall events that are accurately observed as well as under and overobserved. For all but a very few time steps, the uncertainty bounds estimated by this methodology cover the observed rainfall volumes. Considering that all of these rainfall estimates simulate streamflow that is closer to the observed streamflow, this result is quite significant. This indicates that a significant improvement in streamflow simulation can be made with an improved understanding of rainfall uncertainty. A limitation of this methodology is made evident by examining the constant uncertainty bounds for consecutive days. This is an artefact generated by estimating DWT parameters that apply to a number of consecutive days. The impact on the results can be minimized by increasing the number of estimated parameters or by choosing a more suitable analysis wavelet. The study of this issue is outside the scope of this work.

Figure 4 (bottom) shows the converged rainfall volumes for experiments 2 and 3 and the results of a traditional calibration approach in experiment 1. When compared to the synthetic case study in Figure 4 (top), the observation case study in the Figure 4 (bottom) shows that both the independent estimation of rainfall time series and model parameters (experiment 2) and the simultaneous estimation of rainfall time series and model parameter distributions are able to yield rainfall time series that are generally in agreement with the gauges and consistently produce superior streamflow estimates than their respective benchmarks. Further, as seen in Figure 4, the total volumes of the rainfall time series that are estimated in experiments 2 and 3 cover a broad volumetric range. This range is much closer to the range observed at the gauges than their synthetic case study equivalents. The results of experiment 3 indicate that the proposed likelihood function is able to both realistically constrain rainfall estimations and simulate streamflow with RMSE 1.67 times lower than that obtained from only estimating model parameters. Thus, the use of the proposed likelihood function is advantageous when compared to likelihood functions that do not consider input uncertainty.

10.1002/2017WR020442

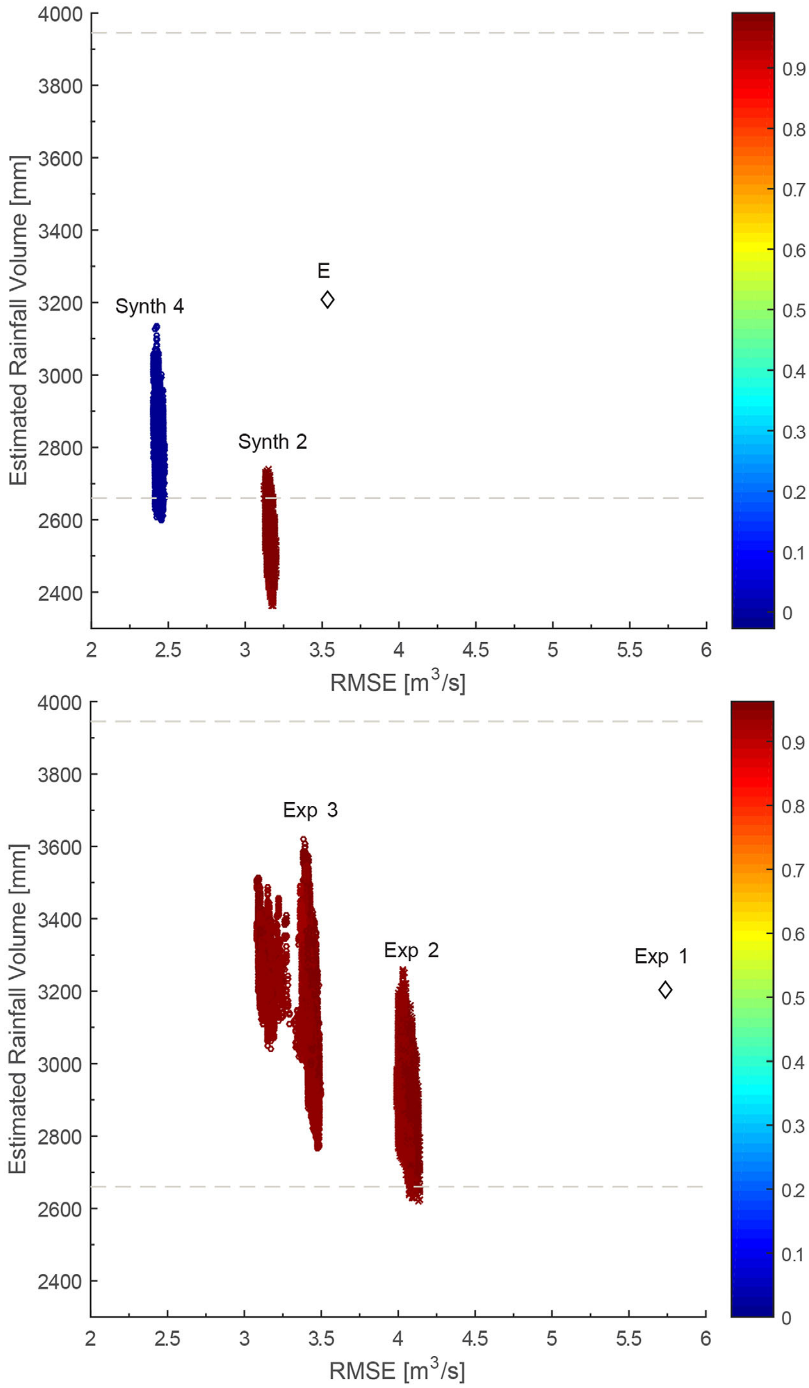

Figure 4. The estimated rainfall volume for the calibration period plotted against the RMSE of the estimated rainfall's streamflow simulation when compared to observed streamflow. The color bar indicates the correlation coefficient between the estimated rainfall and observed rainfall and the dotted lines in both plots show the maximum and minimum rainfall volumes observed at the gauges within the catchment. (top) The estimated rainfall time series after the convergence criteria has been met for Synth 2 and Synth 4. "E" represents the streamflow simulation in which the perturbed rainfall is used as input to the hydrological model with the synthetic truth parameters. (bottom) The same as the top plot but for experiments 2 and 3. Experiment 1 results are shown to demonstrate the results of a traditional calibration approach.

The observation case study further explored some of the different model input data reduction techniques that wavelets make available. In contrast to the synthetic case study, neither the db1 nor db2 wavelets were able to better account for errors in the input data. The formulation of a complete description of rainfall errors was outside the scope of this study. However, this result suggests that the input error in the observation case study contains both homoscedastic and heteroscedastic errors and that further exploration is warranted. It was found that estimating the approximation parameters of lower level DWT decompositions were able to provide the most realistic rainfall time series with streamflow simulations that are superior to the traditional calibration approach. Both a segmented rainfall and model parameter estimation approach and the simultaneous estimation of rainfall and model parameters were able to estimate realistic rainfall time series that simulated streamflow better than the benchmark. The findings detailed in this discussion indicate that using the proposed likelihood function, realistic rainfall time series and streamflow simulations can be obtained.

10. Conclusions

The DWT was used to reduce model input data for the estimation of input uncertainty. Along with DREAM$_{(ZS)}$, different aspects and configurations of the DWT were explored to outline possible methodologies that may be used to estimate input uncertainty. In this study, the methodologies are applied to a gauge-based rainfall estimate yet the methodologies are not limited to gauge-based rainfall estimates. These methodologies could be applied to hydrologic input data such as high-resolution remote sensing of rainfall or even evapotranspiration. It was found that in conjunction with the estimation of DWT rainfall parameters the use of a likelihood function that considers both input rainfall and streamflow error is able to estimate model parameter distributions and entire rainfall time series. The joint estimation of model and wavelet approximation parameters yielded estimates of the most realistic rainfall time series. At the same time, streamflow simulations were shown to have improved RMSE by a factor of up to 1.78 when being compared to benchmark simulations in which only model parameters were estimated. The choice of analysis wavelet used for estimation purposes can have a considerable impact on the errors that are corrected for. In most cases, but not all, the proposed likelihood function was able to effectively constrain rainfall estimations whilst simultaneously producing streamflow simulations that were superior to a traditional calibration approach. Finally, a methodology to create a set of realistic rainfall time series was presented. This methodology will be used in a future study to compare rainfall time series and their respective model parameters with their ability to simulate streamflow and soil moisture observations.

Acknowledgments
The authors would like to extend their gratitude to Jasper Vrugt and the anonymous reviewers for their comments and recommendations. The authors would also like to thank the Bureau of Meteorology (www.bom.gov.au/climate/data) for the provision of data. This work was supported by the Multi-modal Australian ScienceS Imaging and Visualisation Environment (MASSIVE) (www.massive.org.au), a Monash University Engineering Research Living Allowance stipend, and a top up scholarship from the Bushfire & Natural Hazards Cooperative Research Centre. Valentijn Pauwels is funded by ARC grant FT130100545.

References

Abera, W., L. Brocca, and R. Rigon (2016), Comparative evaluation of different satellite rainfall estimation products and bias correction in the Upper Blue Nile (UBN) basin, *Atmos. Res.*, *178–179*, 471–483, doi:10.1016/j.atmosres.2016.04.017.

Adamovic, M., I. Braud, F. Branger, and J. Kirchner (2015), Assessing the simple dynamical systems approach in a Mediterranean context: Application to the Arèche catchment (France), *Hydrol. Earth Syst. Sci.*, *19*(5), 2427–2449, doi:10.5194/hess-19-2427-2015.

Ajami, N., Q. Duan, and S. Sorooshian (2007), An integrated hydrologic Bayesian multimodel combination framework: Confronting input, parameter, and model structural uncertainty in hydrologic prediction, *Water Resour. Res.*, *43*, W01403, doi:10.1029/2005WR004745.

Anderson, R., V. Koren, and S. Reed (2006), Using SSURGO data to improve Sacramento model a priori parameter estimates, *J. Hydrol.*, *320*(1–2), 103–116, doi:10.1016/j.jhydrol.2005.07.020.

Beven, K. (2006), A manifesto for the equifinality thesis, *J. Hydrol.*, *320*(1–2), 18–36, doi:10.1016/j.jhydrol.2005.07.007.

Blazkova, S., and K. Beven (2009), A limits of acceptability approach to model evaluation and uncertainty estimation in flood frequency estimation by continuous simulation: Skalka catchment, Czech Republic, *Water Resour. Res.*, *45*, W00B16, doi:10.1029/2007WR006726.

Boyle, D., H. Gupta, and S. Sorooshian (2000), Toward improved calibration of hydrologic models: Combining the strengths of manual and automatic methods, *Water Resour. Res.*, *36*(12), 3663–3674, doi:10.1029/2000WR900207.

Brocca, L., L. Ciabatta, C. Massari, T. Moramarco, S. Hahn, S. Hasenauer, R. Kidd, W. Dorigo, W. Wagner, and V. Levizzani (2014), Soil as a natural rain gauge: Estimating global rainfall from satellite soil moisture data, *J. Geophys. Res. Atmos.*, *119*, 5128–5141, doi:10.1002/2014JD021489.

Brouwer, R., and R. Van Ek (2004), Integrated ecological, economic and social impact assessment of alternative flood control policies in the Netherlands, *Ecol. Econ.*, *50*(1–2), 1–21.

Bulygina, N., and H. Gupta (2011), Correcting the mathematical structure of a hydrological model via Bayesian data assimilation, *Water Resour. Res.*, *47*, W05514, doi:10.1029/2010WR009614.

Butts, M., J. Payne, M. Kristensen, and H. Madsen (2004), An evaluation of the impact of model structure on hydrological modelling uncertainty for streamflow simulation, *J. Hydrol.*, *298*(1–4), 242–266, doi:10.1016/j.jhydrol.2004.03.042.

Ciabatta, L., L. Brocca, C. Massari, T. Moramarco, S. Puca, A. Rinollo, S. Gabellani, and W. Wagner (2015), Integration of satellite soil moisture and rainfall observations over the Italian territory, *J. Hydrometeorol.*, *16*, 1341–1355, doi:10.1175/JHM-D-14-0108.1.

Clark, M., S. Gangopadhyay, L. Hay, B. Rajagopalan, and R. Wilby (2004), The schaake shuffle: A method for reconstructing space-time variability in forecasted precipitation and temperature fields, *J. Hydrometeorol.*, *5*(1), 243–262.

Crow, W., and D. Ryu (2009), A new data assimilation approach for improving runoff prediction using remotely-sensed soil moisture retrievals, *Hydrol. Earth Syst. Sci.*, *13*(1), 1–16.

Crow, W., M. Van Den Berg, G. Huffman, and T. Pellarin (2011), Correcting rainfall using satellite-based surface soil moisture retrievals: The Soil Moisture Analysis Rainfall Tool (SMART), *Water Resour. Res.*, *47*, W08521, doi:10.1029/2011WR010576.

Crow, W. T. (2007), A novel method for quantifying value in spaceborne soil moisture retrievals, *J. Hydrometeorol.*, *8*(1), 56–67.

Crow, W. T., G. J. Huffman, R. Bindlish, and T. J. Jackson (2009), Improving satellite-based rainfall accumulation estimates using spaceborne surface soil moisture retrievals, *J. Hydrometeorol.*, *10*(1), 199–212.

Daubechies, I. (1990), The wavelet transform, time-frequency localization and signal analysis, *IEEE Trans. Inf. Theory*, *36*(5), 961–1005, doi:10.1109/18.57199.

Duan, Q., S. Sorooshian, and V. K. Gupta (1994), Optimal use of the sce-ua global optimization method for calibrating watershed models, *J. Hydrol.*, *158*(3–4), 265–284.

Elliott, J. (1997), Development of an improved real-time flood forecasting model, technical report Industry report series 1997-06, Coop. Res. Cent. for Catchment Hydrol., Clayton.

Entekhabi, D., et al. (2010), The Soil Moisture Active Passive (SMAP) mission, *Proc. IEEE*, *98*(5), 704–716, doi:10.1109/JPROC.2010.2043918.

Gan, T. Y., and G. F. Biftu (1996), Automatic calibration of conceptual rainfall-runoff models: Optimization algorithms, catchment conditions, and model structure, *Water Resour. Res.*, *32*(12), 3513–3524.

Gelman, A., and D. B. Rubin (1992), Inference from iterative simulation using multiple sequences, *Stat. Sci.*, *7*(4), 457–472, doi:10.1214/ss/1177011136.

Grayson, R. B., A. W. Western, J. P. Walker, D. D. Kandel, J. F. Costelloe, and D. J. Wilson (2006), Controls on patterns of soil moisture in arid and semi-arid systems, in *Dryland Ecohydrology*, pp. 109–127, Springer, Netherlands.

Hajkowicz, S., and K. Collins (2007), A review of multiple criteria analysis for water resource planning and management, *Water Resour. Manage.*, *21*(9), 1553–1566, doi:10.1007/s11269-006-9112-5.

Hapuarachchi, H., Q. Wang, and T. Pagano (2011), A review of advances in flash flood forecasting, *Hydrol. Processes*, *25*(18), 2771–2784.

Herron, N., R. Davis, and R. Jones (2002), The effects of large-scale afforestation and climate change on water allocation in the Macquarie River catchment, NSW, Australia, *J. Environ. Manage.*, *65*(4), 369–381, doi:10.1016/S0301-4797(02)90562-1.

Hino, M. (1986), Improvements in the inverse estimation method of effective rainfall from runoff, *J. Hydrol.*, *83*(1–2), 137–147.

Hou, A., R. Kakar, S. Neeck, A. Azarbarzin, C. Kummerow, M. Kojima, R. Oki, K. Nakamura, and T. Iguchi (2014), The global precipitation measurement mission, *Bull. Am. Meteorol. Soc.*, *95*(5), 701–722, doi:10.1175/BAMS-D-13-00164.1.

Kavetski, D., G. Kuczera, and S. Franks (2006a), Bayesian analysis of input uncertainty in hydrological modeling: 2. Application, *Water Resour. Res.*, *42*, W03408, doi:10.1029/2005WR004376.

Kavetski, D., G. Kuczera, and S. Franks (2006b), Bayesian analysis of input uncertainty in hydrological modeling: 1. Theory, *Water Resour. Res.*, *42*, W03407, doi:10.1029/2005WR004368.

Kirchner, J. (2009), Catchments as simple dynamical systems: Catchment characterization, rainfall-runoff modeling, and doing hydrology backward, *Water Resour. Res.*, *45*, W02429, doi:10.1029/2008WR006912.

Kucera, P. A., E. E. Ebert, F. J. Turk, V. Levizzani, D. Kirschbaum, F. J. Tapiador, A. Loew, and M. Borsche (2013), Precipitation from space: Advancing earth system science, *Bull. Am. Meteorol. Soc.*, *94*(3), 365–375.

Kuczera, G., D. Kavetski, S. Franks, and M. Thyer (2006), Towards a Bayesian total error analysis of conceptual rainfall-runoff models: Characterising model error using storm-dependent parameters, *J. Hydrol.*, *331*(1–2), 161–177, doi:10.1016/j.jhydrol.2006.05.010.

Laloy, E., and J. Vrugt (2012), High-dimensional posterior exploration of hydrologic models using multiple-try DREAM (ZS) and high-performance computing, *Water Resour. Res.*, *48*, W01526, doi:10.1029/2011WR010608.

Mallat, S. (1989), A theory for multiresolution signal decomposition: The wavelet representation, *IEEE Trans. Pattern Anal. Mach. Intel.*, *11*(7), 674–693, doi:10.1109/34.192463.

Mallat, S. (2009), *A Wavelet Tour of Signal Processing*., Academic Press, Boston, Mass.

McMillan, H., B. Jackson, M. Clark, D. Kavetski, and R. Woods (2011), Rainfall uncertainty in hydrological modelling: An evaluation of multiplicative error models, *J. Hydrol.*, *400*(1–2), 83–94.

NWS (2002), *Conceptualization of the Sacramento Soil Moisture Accounting Model*., Silver Spring.

Oudin, L., C. Perrin, T. Mathevet, V. Andréassian, and C. Michel (2006), Impact of biased and randomly corrupted inputs on the efficiency and the parameters of watershed models, *J. Hydrol.*, *320*(1–2), 62–83, doi:10.1016/j.jhydrol.2005.07.016.

Pagano, T., P. Hapuarachchi, and Q. Wang (2009), Continuous soil moisture accounting and routing modelling to support short lead- time streamflow forecasting, technical report EP11464, CSIRO: Water for a Healthy Country Natl. Res. Flagship, Clayton south, doi:10.4225/08/58557d90e8885.

Pappenberger, F., and K. Beven (2006), Ignorance is bliss: Or seven reasons not to use uncertainty analysis, *Water Resour. Res.*, *42*, W05302, doi:10.1029/2005WR004820.

Peck, E. (1976), Catchment modeling and initial parameter estimation for the National Weather Service river forecast system, *NOAA Tech Memo. NWS hydro-31*, Natl. Weather Serv., Silver Spring, Md.

Pellarin, T., A. Ali, F. Chopin, I. Jobard, and J.-C. Bergès (2008), Using spaceborne surface soil moisture to constrain satellite precipitation estimates over West Africa, *Geophys. Res. Lett.*, *35*, L02813, doi:10.1029/2007GL032243.

Pellarin, T., S. Louvet, C. Gruhier, G. Quantin, and C. Legout (2013), A simple and effective method for correcting soil moisture and precipitation estimates using AMSR-E measurements, *Remote Sens. Environ.*, *136*, 28–36.

Renard, B., D. Kavetski, G. Kuczera, M. Thyer, and S. Franks (2010), Understanding predictive uncertainty in hydrologic modeling: The challenge of identifying input and structural errors, *Water Resour. Res.*, *46*, W05521, doi:10.1029/2009WR008328.

Renard, B., D. Kavetski, E. Leblois, M. Thyer, G. Kuczera, and S. Franks (2011), Toward a reliable decomposition of predictive uncertainty in hydrological modeling: Characterizing rainfall errors using conditional simulation, *Water Resour. Res.*, *47*, W11516, doi:10.1029/2011WR010643.

Robertson, D., D. Shrestha, and Q. Wang (2013), Post-processing rainfall forecasts from numerical weather prediction models for short-term streamflow forecasting, *Hydrol. Earth Syst. Sci.*, *17*(9), 3587–3603, doi:10.5194/hess-17-3587-2013.

Rusjan, S., and M. Mikoš (2015), A catchment as a simple dynamical system: Characterization by the streamflow component approach, *J. Hydrol.*, *527*, 794–808, doi:10.1016/j.jhydrol.2015.05.050.

Sadegh, M., and J. Vrugt (2014), Approximate Bayesian computation using Markov Chain Monte Carlo simulation: DREAM(ABC), *Water Resour. Res.*, *50*, 6767–6787, doi:10.1002/2014WR015386.

Samain, B., and V. Pauwels (2013), Impact of potential and (scintillometer-based) actual evapotranspiration estimates on the performance of a lumped rainfall-runoff model, *Hydrol. Earth Syst. Sci.*, *17*(11), 4525–4540, doi:10.5194/hess-17-4525-2013.

Shrestha, D., D. Robertson, J. Bennett, and Q. Wang (2015), Improving precipitation forecasts by generating ensembles through postprocessing, *Mon. Weather Rev.*, *143*(9), 3642–3663, doi:10.1175/MWR-D-14-00329.1.

Teuling, A., I. Lehner, J. Kirchner, and S. Seneviratne (2010), Catchments as simple dynamical systems: Experience from a Swiss prealpine catchment, *Water Resour. Res.*, *46*, W10502, doi:10.1029/2009WR008777.

Thiemann, M., M. Trosset, H. Gupta, and S. Sorooshian (2001), Bayesian recursive parameter estimation for hydrologic models, *Water Resour. Res.*, *37*(10), 2521–2535.

Thyer, M., G. Kuczera, and B. C. Bates (1999), Probabilistic optimization for conceptual rainfall-runoff models: A comparison of the shuffled complex evolution and simulated annealing algorithms, *Water Resour. Res.*, *35*(3), 767–773.

Thyer, M., B. Renard, D. Kavetski, G. Kuczera, S. Franks, and S. Srikanthan (2009), Critical evaluation of parameter consistency and predictive uncertainty in hydrological modeling: A case study using Bayesian total error analysis, *Water Resour. Res.*, *45*, W00B14, doi:10.1029/2008WR006825.

Vrugt, J. (2016), Markov chain Monte Carlo simulation using the DREAM software package: Theory, concepts, and MATLAB implementation, *Environ. Modell. Software*, *75*, 273–316, doi:10.1016/j.envsoft.2015.08.013.

Vrugt, J. A., and B. Robinson (2007), Treatment of uncertainty using ensemble methods: Comparison of sequential data assimilation and Bayesian model averaging, *Water Resour. Res.*, *43*, W01411, doi:10.1029/2005WR004838.

Vrugt, J. A., and C. Ter Braak (2011), DREAM(D): An adaptive Markov Chain Monte Carlo simulation algorithm to solve discrete, noncontinuous, and combinatorial posterior parameter estimation problems, *Hydrol. Earth Syst. Sci.*, *15*(12), 3701–3713, doi:10.5194/hess-15-3701-2011.

Vrugt, J. A., C. Diks, H. Gupta, W. Bouten, and J. Verstraten (2005), Improved treatment of uncertainty in hydrologic modeling: Combining the strengths of global optimization and data assimilation, *Water Resour. Res.*, *41*, W01017, doi:10.1029/2004WR003059.

Vrugt, J. A., C. Ter Braak, M. Clark, J. Hyman, and B. Robinson (2008), Treatment of input uncertainty in hydrologic modeling: Doing hydrology backward with Markov Chain Monte Carlo simulation, *Water Resour. Res.*, *44*, W00B09, doi:10.1029/2007WR006720.

Vrugt, J. A., C. ter Braak, H. Gupta, and B. Robinson (2009a), Equifinality of formal (DREAM) and informal (GLUE) Bayesian approaches in hydrologic modeling?, *Stochastic Environ. Res. Risk Assess.*, *23*(7), 1011–1026, doi:10.1007/s00477-008-0274-y.

Vrugt, J. A., C. J. F. ter Braak, C. G. H. Diks, B. A. Robinson, J. M. Hyman, and D. Higdon (2009b), Accelerating Markov chain Monte Carlo simulation by differential evolution with self-adaptive randomized subspace sampling, *Int. J. Nonlinear Sci. Numer. Simul.*, *10*(3), 273–290.

Wright, A., J. P. Walker, D. E. Robertson, and V. R. N. Pauwels (2017), A comparison of the Discrete Cosine and Wavelet Transforms for hydrologic model input data reduction, *Hydrol. Earth Syst. Sci. Discuss.*, *21*, 3827–3838, doi:10.5194/hess-2017-26.

Young, P. (2013), Hypothetico-inductive data-based mechanistic modeling of hydrological systems, *Water Resour. Res.*, *49*, 915–935, doi:10.1002/wrcr.20068.